Hormonally Mediated Increases in Sex-Biased Gene Expression Accompany the Breakdown of Between-Sex Genetic Correlations in a Sexually Dimorphic Lizard

Robert M. Cox,[1,*,†] Christian L. Cox,[1,2,*] Joel W. McGlothlin,[3] Daren C. Card,[4] Audra L. Andrew,[4] and Todd A. Castoe[4]

1. Department of Biology, University of Virginia, Charlottesville, Virginia 22904; 2. Department of Biology, Georgia Southern University, Statesboro, Georgia 30460; 3. Department of Biological Sciences, Virginia Tech, Blacksburg, Virginia 24061; 4. Department of Biology, University of Texas at Arlington, Arlington, Texas 76019

Submitted July 16, 2016; Accepted October 7, 2016; Electronically published January 25, 2017

Online enhancements: appendix. *Dryad data:* http://dx.doi.org/10.5061/dryad.n95k3.

ABSTRACT: The evolution of sexual dimorphism is predicted to occur through reductions in between-sex genetic correlations (r_{mf}) for shared traits, but the physiological and genetic mechanisms that facilitate these reductions remain largely speculative. Here, we use a paternal half-sibling breeding design in captive brown anole lizards (*Anolis sagrei*) to show that the development of sexual size dimorphism is mirrored by the ontogenetic breakdown of r_{mf} for body size and growth rate. Using transcriptome data from the liver (which integrates growth and metabolism), we show that sex-biased gene expression also increases dramatically between ontogenetic stages bracketing this breakdown of r_{mf}. Ontogenetic increases in sex-biased expression are particularly evident for genes involved in growth, metabolism, and cell proliferation, suggesting that they contribute to both the development of sexual dimorphism and the breakdown of r_{mf}. Mechanistically, we show that treatment of females with testosterone stimulates the expression of male-biased genes while inhibiting the expression of female-biased genes, thereby inducing male-like phenotypes at both organismal and transcriptomic levels. Collectively, our results suggest that sex-specific modifiers such as testosterone can orchestrate sex-biased gene expression to facilitate the phenotypic development of sexual dimorphism while simultaneously reducing genetic correlations that would otherwise constrain the independent evolution of the sexes.

Keywords: Anolis, animal model, body size, intralocus sexual conflict, quantitative genetics, testosterone, transcriptome.

Introduction

All species with separate sexes face a common challenge: distinct male and female phenotypes must be produced from an underlying genome that is almost entirely shared between the sexes. This genomic constraint is expected to hinder the independent evolution of males and females toward their respective phenotypic optima, thereby reducing the fitness of populations in a phenomenon known as intralocus sexual conflict (Rice and Chippindale 2001; Bonduriansky and Chenoweth 2009; Cox and Calsbeek 2009). From the perspective of quantitative genetics, the resolution of this genomic conflict is predicted to occur through gradual evolutionary reductions in the between-sex genetic correlations (r_{mf}) for shared phenotypic traits (Lande 1980, 1987; Fairbairn and Roff 2006). Consistent with theory, the magnitude of r_{mf} negatively correlates with the degree of sexual dimorphism across diverse traits and species (Poissant et al. 2010), and artificial selection against between-sex genetic covariance can reduce r_{mf} within a few generations (Delph et al. 2011). However, translating mathematical descriptors such as r_{mf} into mechanistic explanations of how genetic correlations are structured and how they evolve at the molecular level remains an outstanding challenge in evolutionary genetics (Badyaev 2002; Bonduriansky and Rowe 2005; Fairbairn and Roff 2006; Stocks et al. 2015).

The evolution of sexual dimorphism and corresponding resolution of intralocus sexual conflict can be facilitated by a variety of genetic mechanisms, including sex linkage (van Doorn and Kirkpatrick 2007; Roberts et al. 2009), sex-specific transcript splicing (Stewart et al. 2010; Kijimoto et al. 2012), genomic imprinting (Day and Bonduriansky 2004; Bonduriansky 2007), and gene duplication (Connallon and Clark 2011; Gallach and Betrán 2011). Given that the majority of genes typically reside on autosomes, sex-biased expression of these shared genes is predicted to be a mechanism of general importance in the resolution of sexual conflict (Ellegren and Parsch 2007; Mank 2009; Innocenti and

* These authors served as lead authors and contributed equally to this work.
† Corresponding author; e-mail: rmc3u@virginia.edu.

ORCIDs: R. M. Cox, http://orcid.org/0000-0001-8325-111X; McGlothlin, http://orcid.org/0000-0003-3645-6264; Card, http://orcid.org/0000-0002-1629-5726.

Am. Nat. 2017. Vol. 189, pp. 315–332.
DOI: 10.1086/690105

Morrow 2010; Mank et al. 2010; Ingleby et al. 2015; Grath and Parsch 2016). Several studies hint that the degree of sex-biased gene expression is associated with the magnitude of sexual dimorphism (Pointer et al. 2013; Harrison et al. 2015) and of sexual conflict (Hollis et al. 2014). Moreover, genes with sex-biased expression tend to have lower correlations between male and female expression levels when measured across populations or species (Dean and Mank 2016) and lower r_{mf} for expression when measured within populations (Griffin et al. 2013). However, the extent to which sex differences in gene expression contribute to the reduction of r_{mf} for sexually dimorphic phenotypes is not known (Badyaev 2002).

Insight into the relationship between sex-biased gene expression and r_{mf} for sexually dimorphic phenotypes may be gained by tracing their concomitant developmental trajectories within a single population. A meta-analysis of data from a variety of taxa indicates that r_{mf} tends to decrease throughout ontogeny as sexual dimorphism develops (Poissant and Coltman 2009), though most of the studies reviewed therein measured r_{mf} at only two or three ontogenetic stages and were conducted in aquacultural, agricultural, or medical frameworks with limited consideration of evolutionary theory (but see Parker and Garant 2005). A separate body of work indicates that sex-biased gene expression tends to increase as ontogeny progresses (Mank et al. 2010; Magnusson et al. 2011; Zhao et al. 2011; Ingleby et al. 2015), suggesting that ontogenetic reductions in r_{mf} may be driven by developmental increases in sex-biased gene expression. However, studies of the ontogeny of r_{mf} and of sex-biased gene expression have yet to be conducted across the same developmental trajectory in the same species. Moreover, most ontogenetic studies of sex-biased gene expression have focused on broad transcriptional patterns with limited consideration of underlying mechanistic pathways and their potential links to sexually dimorphic phenotypes. This lack of information on the underlying mechanism and on concurrent ontogenetic changes in both r_{mf} and sex-biased gene expression within a single system represents a gap in our ability to synthesize quantitative genetic and transcriptomic perspectives on the evolution of sexual dimorphism.

Identifying the functional pathways that become sex biased during ontogeny not only helps to link expression phenotypes to organismal phenotypes for which r_{mf} is characterized but can also facilitate direct tests of mechanisms that coordinate sex-biased expression of genes and phenotypes. In vertebrates, many of the developmental changes in sex-biased gene expression that are hypothesized to reduce r_{mf} may be coordinated by epigenetic modifiers such as sex steroids (van Nas et al. 2009), which are produced by the sexually differentiated gonads and then circulated to diverse target tissues to bind nuclear receptors and alter transcription. As such, sex steroids may often facilitate the resolution of intralocus sexual conflict by mediating the sex-specific expression of shared genes (Mills et al. 2012; Mokkonen et al. 2012; Peterson et al. 2013, 2014). The basic elements of this idea were laid out by Fisher (1930), who proposed that the "internal secretions of the sexual glands" (i.e., sex steroids) should lead to increasingly sex-specific patterns of genetic variance as ontogeny progresses. Despite increasing focus on the ontogeny of sex-biased gene expression (Mank et al. 2010; Perry et al. 2014; Ingleby et al. 2015; Grath and Parsch 2016) and ontogenetic changes in the quantitative-genetic architecture underlying sexual dimorphism (Badyaev 2002; Parker and Garant 2005; Poissant and Coltman 2009; Chou et al. 2016), we still know relatively little about how sex steroids fit into this picture (Mank 2007; van Nas et al. 2009; Peterson et al. 2013, 2014). By contrast, we know a great deal about how these hormones shape the development of phenotypic sexual dimorphism, particularly in the focal species for this study, where testosterone is known to induce male-like patterns of growth, metabolism, energetics, and ornamentation in juvenile females (Cox et al. 2015).

In this study, we combine quantitative genetic analyses, transcriptomics, and hormone manipulations to provide an integrative perspective on the ontogeny of sexual size dimorphism in the brown anole, *Anolis sagrei*. This small lizard exhibits extreme male-biased sexual size dimorphism that develops gradually over ontogeny, and it has been the focus of extensive research on intralocus sexual conflict (Calsbeek and Bonneaud 2008; Cox and Calsbeek 2010*a*, 2010*b*). First, we test whether sexual size dimorphism in *A. sagrei* is associated with a reduction in r_{mf} for body size and whether r_{mf} decreases as sexual dimorphism develops during ontogeny. In doing this, we develop the most ontogenetically detailed characterization of r_{mf} and its underlying components of within- and between-sex genetic variance and covariance to date and then use these data to identify appropriate ontogenetic stages at which to test for associated changes in sex-biased gene expression. We next analyze transcriptomes from the liver (which integrates growth and metabolism) at two stages bracketing the decline of r_{mf} to test whether genome-wide patterns of sex-biased gene expression increase as r_{mf} breaks down and whether ontogenetic increases in sex-biased gene expression are particularly evident for genes and pathways involved in growth, metabolism, and cell proliferation. Last, to determine the extent to which these ontogenetic changes in sex-biased gene expression are mediated by sex-specific endocrine modifiers, we treat juvenile females with testosterone to test whether this hormone pleiotropically induces patterns of gene expression that are characteristic of males during sexual divergence in growth, gene expression, and genetic architecture. Our results reveal pronounced ontogenetic increases in the sex-biased expres-

sion of growth-regulatory genes that accompany the reduction of r_{mf} and suggest that these changes, many of which are inducible by testosterone, may help to break down the underlying genetic correlations that would otherwise constrain the independent evolution of males and females.

Methods

Breeding Design and Phenotypes

We collected *Anolis sagrei* adults from Great Exuma, the Bahamas (23°29′N, 75°45′W), and transported them to the University of Virginia. We housed each adult individually in its own plastic cage (males: 40 cm × 23 cm × 32 cm; females: 30 cm × 20 cm × 20 cm; Lee's Kritter Keeper, San Marcos, CA) containing a carpet substrate, a potted plant for oviposition, a section of PVC pipe for perching and hiding (30-cm length, 2.5-cm diam.), and a strip of fiberglass screen for basking. We placed each cage beneath two Repti-Sun 10.0 UVB bulbs (ZooMed, San Luis Obispo, CA) and housed all cages in a room set to maintain constant temperature (29°C), relative humidity (65%), and photoperiod (12L:12D during simulated winter, 13L:11D during the breeding season). Three times per week we offered each male five to seven large (1/2-inch) crickets (*Gryllus assimilis* and *Gryllodes sigillatus*; Ghann's Cricket Farm, Augusta, GA) and each female three to five medium-sized (3/8-inch) crickets, dusted weekly with Fluker's Reptile Vitamin and Calcium supplements (Fluker's Cricket Farms, Port Allen, LA). We sprayed cage walls and potted plants twice daily with deionized water for drinking and to maintain a humid microenvironment.

For breeding, we introduced a female into the cage of a male and allowed the pair to mate ad lib. for 14 days before returning the female to her own cage. To generate paternal half-siblings, we repeated this procedure by introducing a second female into the cage of the same male 7 days after removal of the first female. Thereafter, we housed females in isolation and checked the potted plant in each female's cage once per week for new eggs. Anoles lay single eggs every 7–14 days and produce viable eggs from stored sperm for several months following a single mating (Cox and Calsbeek 2010*a*), so we recreated each pairing every 4–6 months to prevent sperm limitation. In total, these pairings produced 429 male and 460 female offspring from 62 sires and 103 dams. We transplanted each new egg to an individual plastic container filled with moist vermiculite (1:1 deionized water to vermiculite by mass) and then incubated these containers at 28°C, 80% relative humidity, and a 12L:12D photoperiod in a Percival Intellus 136VL. We checked containers twice daily for new hatchlings, which we immediately sexed (females exhibit a dorsal pattern that is absent in males), massed, assigned a toe clip for permanent identification, and housed individually in cages identical to those of adult females. We offered each hatchling 10–15 pinhead crickets daily (*Acheta domestica*, bred from adults from Fluker's Cricket Farms; dusted daily with Fluker's Reptile Vitamin and Calcium). At 3 months, we began offering each juvenile two or three small (1/4-inch) crickets (*G. sigillatus*) three times per week (dusted weekly). At 12 months, when the sexes had diverged in size and appetite, we began offering males five to seven large (1/2-inch) crickets and females three to five medium-sized (3/8-inch) crickets three times per week (dusted weekly). Although this sex-specific diet created a different growth environment for each sex, we carefully selected these regimens to approximate ad lib. feeding for both sexes despite differences in the absolute amount of food available to each, a practical necessity given the dramatically different growth trajectories and body sizes of *A. sagrei* males and females.

We measured body mass and collected radiographs for each captive-bred individual at 1, 3, 6, 9, 12, and 24 months posthatching. We made radiographs by placing each animal in a small plastic bag with pinholes for ventilation, cooling the animal for 10 min at 5°C, and then arranging it in a standardized posture on radiograph film (Kodak Biomax XAR). We made exposures at 20–28 kV for 12 s in a Faxitron 43805N or MX-20 radiography system and developed film in an SRX-101A medical film processor (Konica Minolta, Tokyo). We scanned each radiograph to produce a digital image (fig. 1*A*) and used ImageJ software (Schneider et al. 2012) to measure the length of each animal from the tip of the rostrum to the intersection of the sacral and caudal vertebrae, which approximates snout-vent length (SVL). We tested for sex differences in body size at each age using general linear models with SVL or mass as a response variable, sex as a fixed effect, age (days posthatching) as a covariate, and sire and dam (nested within sire) as random effects to account for nonindependence of full and half-siblings. We tested for sex differences in growth using the rate of change in SVL (in millimeters per day) or mass (in grams per day) over each sampling interval as the dependent variable and SVL or mass at the beginning of each interval as a covariate, along with random effects of sire and dam (nested within sire).

Quantitative Genetics

We fitted bivariate animal models for the natural log of SVL and the natural log of mass separately at each age (1, 3, 6, 9, 12, and 24 months) using ASReml 4.1 (Gilmour et al. 2015), with male and female values treated as separate traits and age (days posthatching) as a covariate. Each model fitted additive genetic variances for each sex (V_{Am}

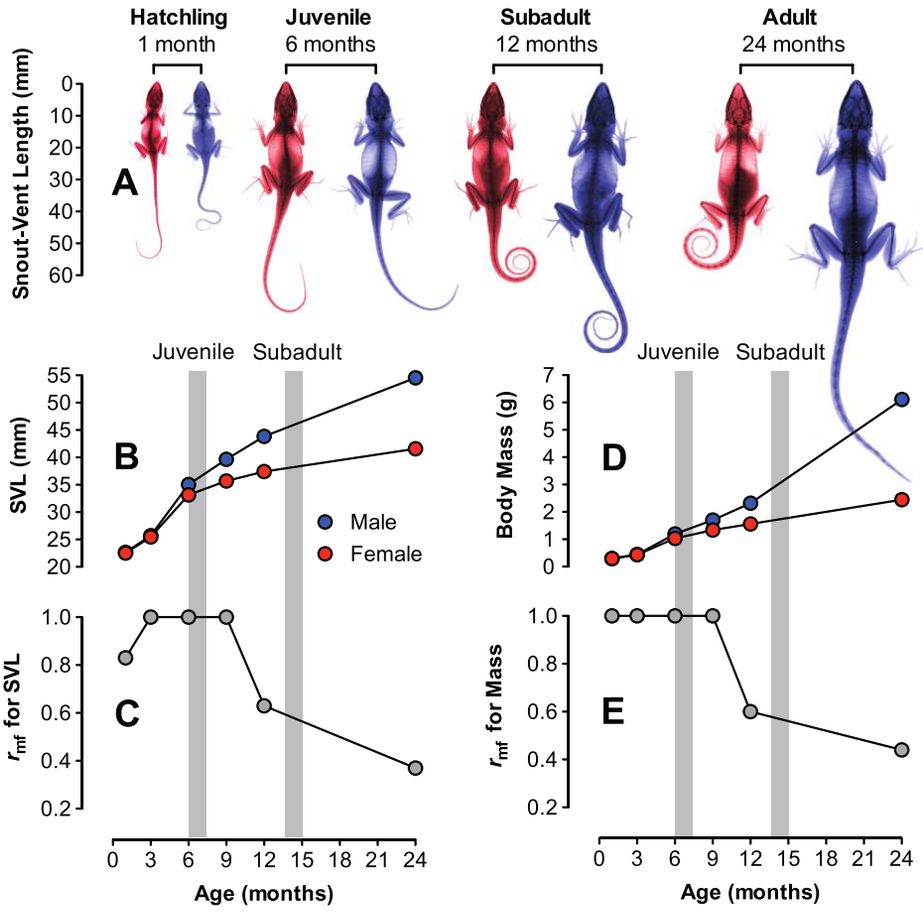

Figure 1: Development of sexual size dimorphism in *Anolis sagrei*. *A*, Representative radiographs of females (red) and males (blue) at each of four ages. Developmental changes in mean snout-vent length (SVL) of males and females (*B*) are mirrored by breakdown of the between-sex genetic correlation (r_{mf}) for SVL (*C*). *D*, *E*, Analogous patterns are shown for body mass. Gray bars indicate the timing of gene expression studies in juveniles and subadults (fig. 2).

and V_{Af}) in addition to r_{mf}. We also calculated the between-sex genetic covariance (B) using the equation

$$B = r_{mf}\sqrt{V_{Am}V_{Af}}.$$

Models including an additional effect of dam (to estimate dominance or maternal effects) did not provide appreciably different results; therefore, to reduce model complexity, we did not include dam effects. We fitted a variety of reduced models with parameters constrained to 0 or 1. Reduced model 1 constrained V_{Am} and r_{mf} to 0, reduced model 2 constrained V_{Af} and r_{mf} to 0, reduced model 3 constrained r_{mf} to 0, and reduced model 4 constrained r_{mf} to 1. We used likelihood-ratio tests with one degree of freedom to assess the statistical significance of each genetic parameter, making the following comparisons: reduced model 3 versus reduced model 1 (H_0: $V_{Am} = 0$), reduced model 3 versus reduced model 2 (H_0: $V_{Af} = 0$), full model versus reduced model 3 (H_0: $r_{mf} = 0$), and full model versus reduced model 4 (H_0: $r_{mf} = 1$). Sex-specific estimates of heritability (h^2) and their standard errors were calculated within ASReml, with statistical significance assessed using *t*-tests. We tested for ontogenetic patterns in V_A, h^2, B, and r_{mf} using the Pearson correlations between each genetic parameter and age in months. As a complementary approach, we also estimated these same quantitative genetic parameters for linear growth rates in SVL (in millimeters per day) and mass (in grams per day) calculated between each measurement interval (1–3, 3–6, 6–9, 9–12, and 12–24 months). Finally, we analyzed the quantitative genetics of growth trajectories estimated across the entire ontogeny by fitting von Bertalanffy growth functions to size data from each individual using the equation

$$\mathrm{SVL}_t = \mathrm{SVL}_\infty(1 - e^{-k(t-t_0)})$$

and then used estimates of asymptotic size (SVL_∞) and the characteristic growth rate (k) from these equations as traits (ln-transformed) in a multivariate animal model. We used

exact age (in days) at each size measurement to calculate growth curves and excluded any individuals lacking size data at 1 or 24 months of age, those with fewer than four total size measurements across ontogeny, and 12 males with estimates of $k < 0.001$, which indicated that growth was approximately linear across ontogeny and therefore yielded unrealistic estimates of $SVL_\infty > 90$ mm. We used likelihood-ratio approaches similar to those described above to assess statistical significance from these models. Data sets for quantitative genetic analyses are available in the Dryad Digital Repository: http://dx.doi.org/10.5061/dryad.n95k3 (Cox et al. 2016*a*).

Testosterone Manipulation

We elevated testosterone in a subset of juvenile females that were 5 or 6 months of age, when sexual dimorphism was first starting to develop, using surgically implanted Silastic tubules containing 100 μg testosterone (methods are detailed elsewhere; Cox et al. 2015). Plasma testosterone levels were weakly sexually dimorphic at this age, and implants significantly elevated testosterone levels of experimental females relative to control animals (receiving a sham surgery and empty implant) of each sex (Cox et al. 2015), but these were well within normal physiological levels observed for maturing and adult males of this species (Cox et al. 2009*a*, 2009*b*). Two months after this manipulation, we assessed gene expression from a subset of these females ($n = 3$) that we selected to match the age of juveniles included in our studies of sex bias (see below) and after confirming elevated testosterone levels in comparison to sham control males ($n = 4$) and females ($n = 3$) of similar age that were also sampled for gene expression. We have previously shown that testosterone induces male-like patterns of growth, energetics, and ornamentation in females of this age (Cox et al. 2015).

Gene Expression

We assessed gene expression in a subset of animals ($n = 4$ per sex) at two time points: 7 months (hereafter, juveniles), when sexual dimorphism was first beginning to develop and decreases in r_{mf} were not yet evident, and 14 months (hereafter, subadults), when sex differences in growth were maximal and r_{mf} was declining rapidly (fig. 1). We removed lizards from their cages and immediately euthanized them by decapitation, excised and weighed their livers, cut each liver into 1-mm^3 pieces, and transferred these pieces into RNAlater (Qiagen, Valencia, CA), storing them at −80°C until extraction of total RNA using TRIzol reagent (Invitrogen). We constructed Illumina mRNAseq multiplexed libraries using NEB Next RNAseq kits (New England Biolabs, Ipswich, MA). We quantified RNAseq libraries using an Agilent BioAnalyzer, pooled libraries in equal molar ratios, and sequenced this pool once on an Illumina MiSeq using 300-bp single-end reads and again on a single Illumina HiSeq 2500 lane using 100-bp paired-end reads.

We demultiplexed the Illumina RNA-seq reads by index and filtered and trimmed them using Trimmomatic v. 0.32 (Bolger et al. 2014) with default settings. We combined reads from different sequencing runs (MiSeq and HiSeq) for the same individual and mapped these reads to the complete annotated transcript set of the congener *Anolis carolinensis* (AnoCar 2.0; Ensembl release 75; Alfioldi et al. 2011) using the MEM algorithm of BWA (Li and Durbin 2009). We used BWA-MEM default parameters, except for a mismatch penalty of 2, a gap penalty of 3, and an alignment output threshold of 20. We analyzed gene expression by counting the number of reads that uniquely mapped to annotated transcripts using SAMtools (Li et al. 2009). We normalized the raw expression data using the TMM method in edgeR (Robinson et al. 2010) and used these normalized counts for all analyses.

Within each age class, we identified genes that were differentially expressed between sexes by conducting pairwise exact tests with a negative binomial distribution corrected for a false discovery rate < 0.05 (Benjamini and Hochberg 1995) in edgeR (Robinson et al. 2010). For the subset of genes ($n = 488$) that these tests identified as differentially expressed between sexes, we visualized patterns of gene expression using the heatmap function in R. We also categorized all of the 15,915 genes that were actively transcribed in each sex into bins ranging from minor (<1.2-fold) to major (>3-fold) sex biases in expression and then tested whether the distribution of genes in each bin was biased in favor of juveniles or subadults using χ^2 tests. We characterized the responsiveness of gene expression to testosterone by conducting pairwise exact tests (as above) between juvenile females receiving blank versus testosterone implants, and we also calculated the $\log_2$ fold difference in expression between these groups for each gene. We then tested whether the direction and magnitude of sex-biased expression in subadults predicted the direction and magnitude of responsiveness to testosterone in juvenile females across the entire set of expressed genes in the liver, across a subset of 466 genes that were significantly sex-biased in subadults, and for 102 genes specifically related to growth, energetics, and cell proliferation (described below). Comparing responsiveness to testosterone in juveniles to sex bias in subadults ensured statistical independence of all calculated fold changes because separate transcriptomes from different individuals were used to quantify dependent and independent variables.

To explore the functional basis of sex differences in gene expression, we used enrichment analyses to identify gene ontology (GO) groups (Ashburner et al. 2000) that were enriched for significantly sex-biased genes. We first used

BioMart (Smedley et al. 2015) to translate *Anolis* Ensembl IDs to human Ensembl IDs, excluding any genes for which we could not identify orthologs. We then conducted GO enrichment analyses for sex-biased genes, using all genes that were expressed in the *A. sagrei* liver as the null background in WebGestalt (Zhang et al. 2005; Wang et al. 2013), with hypergeometric statistical tests and $\alpha = 0.05$ following correction for multiple comparisons (Benjamini and Hochberg 1995). We used ingenuity pathway analysis (IPA; Qiagen) to identify canonical pathways that were significantly enriched for sex-biased genes and to predict the activation states of those pathways. We also used IPA to characterize pathways that were responsive to testosterone, with the caveat that our classification was based on significance at an uncorrected threshold of $\alpha = 0.05$ due to the low number of genes ($n = 28$) that remained significantly responsive to testosterone after correction for the false discovery rate with only $n = 3$ females per treatment group.

As a more targeted approach for quantifying sex-biased expression of genes predicted to be important for growth and body size, we a priori selected three signaling pathways that regulate growth, energetics, and cell proliferation in vertebrates: the growth hormone/insulin-like growth factor (GH/IGF) network, the mechanistic target of rapamycin (mTOR) network, and the insulin-signaling network. We assembled these networks using WikiPathways (Kelder et al. 2011) and the KEGG database (Kanehisa and Goto 2000; Kanehisa et al. 2004). Within each network, we treated each gene ($n = 16$ GH/IGF; $n = 25$ mTOR; $n = 78$ insulin) as an observation and used paired (by gene) Wilcoxon signed-rank tests to determine whether the absolute value of the fold difference in expression between sexes differed between juveniles and subadults (excluding any genes for which mean expression was 0 for any group). We then compared the magnitude of the ontogenetic change in sex bias of growth genes to the baseline change observed across all genes expressed in the liver to determine whether any ontogenetic increases were particularly pronounced for growth genes. We also tested whether the direction of sex bias for these genes in subadults predicted their responsiveness to testosterone in juvenile females ($\log_2$ fold change in expression) using Mann-Whitney tests. We tested for sex differences in expression at each age on a gene-by-gene basis for the subset of 16 genes in the GH/IGF network (under the a priori reasoning that these genes would be most directly related to growth and body size) by asking whether the uncorrected P values derived from pairwise exact tests with a negative binomial distribution in edgeR remained significant following Bonferroni correction for multiple comparisons ($P < .0031$). Last, we compared patterns in expression in these GH/IGF genes among control females, females treated with testosterone, and control males to examine the extent to which testosterone induced male-typical patterns of expression.

Results

Development of Sexual Dimorphism

Sex differences in snout-vent length (SVL) and body mass were negligible at 1 and 3 months, but males grew more quickly than females over every subsequent interval such that males and females differed significantly in size by 6 months and at every age thereafter (fig. 1; table 1). Consequently, the magnitude of phenotypic sexual size dimorphism increased from effectively 0 at 1 month to 31% (SVL) and 172% (mass) by 24 months (fig. 1). Males exceeded females by 51% in asymptotic size estimated from growth trajectories (mean male $\text{SVL}_\infty = 63.8$; mean female $\text{SVL}_\infty = 42.3$; $F = 1,725$; $P < .0001$), whereas females had growth parameters nearly twice as large (mean male $k = 0.0024$; mean female $k = 0.0046$; $F = 795$; $P < .0001$), indicating that females approached SVL_∞ earlier in ontogeny than did males, whereas growth trajectories were relatively more linear and less asymptotic in males.

Developmental Breakdown of Between-Sex Genetic Correlations

Between-sex genetic correlations (r_{mf}) for SVL and body mass were initially high (equal to 1 in all but one case) from 1 to 9 months but had declined sharply by 12 months and had reached values that were significantly lower than 1 by 24 months (table 2; fig. 1). This decline in r_{mf} with age was statistically significant for both SVL and mass (table 3) and was driven by two factors. First, between-sex genetic covariance (B) decreased with age (tables 2, 3). Because the between-sex genetic correlation is defined as

$$r_{\text{mf}} = \frac{B}{\sqrt{V_{\text{Am}} V_{\text{Af}}}},$$

this decrease in the numerator reduced r_{mf} over ontogeny. This decrease in B was significant for SVL but not for mass (table 3). Second, although additive genetic variances for SVL and mass were generally significant and uniform across ontogeny in females (V_{Af}), additive genetic variances in males (V_{Am}) were initially low but increased substantially as ontogeny progressed (tables 2, 3). Appreciable V_{Am} for SVL and mass began to emerge at 12 months, and by 24 months heritability (h^2) estimates for SVL and mass were similar in both sexes (table 2). This increase in V_{Am} (table 3) caused an increase in the denominator of r_{mf} and a corresponding decrease in the absolute value of r_{mf}. Likewise, V_{Af} and h^2 for growth rates in females were low and constant across ontogeny, whereas V_{Am} and h^2 for growth rates in males were low before 9 months but increased thereafter and eventually became significant in adult males between 12 and 24 months

Table 1: Statistical tests for sex differences in body size and growth rate across age classes

			Sex (fixed effect)		Age or size (covariate)	
Phenotype and age (months)	*N*	df	*F*	*P*	*F*	*P*
SVL (mm):						
1	845	1, 822.9	1.90	.1684	25.32	<.0001
3	730	1, 721.3	3.82	.0511	57.96	<.0001
6	719	1, 705.0	340.01	<.0001	155.59	<.0001
9	611	1, 600.2	914.36	<.0001	20.73	<.0001
12	719	1, 706.1	2,142.07	<.0001	.82	.3656
24	577	1, 551.3	5,431.68	<.0001	17.78	<.0001
Mass (g):						
1	863	1, 845.5	.03	.8541	2.60	.1069
3	751	1, 744.4	2.46	.1174	110.06	<.0001
6	740	1, 721.8	228.79	<.0001	122.94	<.0001
9	618	1, 609.0	430.49	<.0001	12.15	.0005
12	722	1, 714.6	944.73	<.0001	6.37	.0118
24	587	1, 569.3	3,644.20	<.0001	24.61	<.0001
Growth in SVL (mm/d):						
1–3	694	1, 687.5	3.08	.0796	30.52	<.0001
3–6	656	1, 648.9	335.09	<.0001	255.78	<.0001
6–9	562	1, 553.0	494.10	<.0001	160.58	<.0001
9–12	554	1, 545.8	362.17	<.0001	50.05	<.0001
12–24	557	1, 547.3	898.20	<.0001	212.47	<.0001
Growth in mass (g/d):						
1–3	729	1, 722.4	1.90	.1690	23.77	<.0001
3–6	693	1, 682.4	215.47	<.0001	42.15	<.0001
6–9	585	1, 471.8	233.83	<.0001	62.11	<.0001
9–12	560	1, 550.0	191.26	<.0001	8.57	.0036
12–24	571	1, 565.5	1,406.14	<.0001	88.37	<.0001

Note: Effects of sex are reported from models with actual age (days since hatching, for analyses of SVL and mass) or initial body size (SVL or mass, for analyses of growth rates) as covariates and random effects of sire and dam (nested within sire), which are not shown here. Degrees of freedom in the numerator and estimated degrees of freedom in the denominator are shown for tests of the sex effect. SVL = snout-vent length.

(table A1; tables A1–A7 are available online). Asymptotic size (SVL_∞) was significantly heritable in males and females and exhibited a moderate r_{mf} that was not significantly different from 0 (table 4). The growth parameter k describing the shape of the trajectory was heritable and genetically correlated with SVL_∞ in males, but it was not heritable in females, and due in part to low V_{Af}, it exhibited a moderately high r_{mf} that was not significantly different from 0 (table 4).

Developmental Increases in Sex-Biased Gene Expression

A total of 488 genes exhibited significantly sex-biased expression, comprising 3.1% of the 15,915 genes that were expressed in the liver transcriptomes of both sexes. Only 15 of these 488 differentially expressed genes map to the X chromosome in *Anolis carolinensis*, such that X-linked genes were only slightly (and not significantly) more likely than autosomal genes to exhibit sex-biased expression ($\chi^2 = 2.92$; $P = .087$) relative to the abundance of each in the genome. There was a sharp ontogenetic increase from 25 sex-biased genes in juveniles (13 female biased, 12 male biased; fig. 2*A*) to 466 sex-biased genes in subadults (177 female biased, 289 male biased; fig. 2*B*). Male-biased genes thus significantly outnumbered female-biased genes in subadults ($\chi^2 = 26.92$; $P < .0001$). Heat maps for these subsets of sex-biased genes emphasize the stark nature of this ontogenetic increase in sex bias (fig. 2*C*, 2*D*). Relative to juveniles, subadults had fewer genes with minor (<1.2-fold) sex differences in expression ($\chi^2 = 174.07$; $P < .0001$), about the same number of genes with moderate (1.2- to 1.5-fold) sex differences in expression ($\chi^2 = 0.48$; $P = .49$, and more genes with larger sex differences of 1.5- to 2-fold ($\chi^2 = 56.99$; $P < .0001$), 2- to 3-fold ($\chi^2 = 126.63$; $P < .0001$), and >3-fold ($\chi^2 = 106.83$; $P < .0001$; fig. 2*E*). The direction and degree of sex-biased expression in juveniles ($\log_2$ fold difference) was weakly positively correlated with that in subadults when assessed across all 15,915 genes that were expressed in both sexes ($r = 0.101$; $P < .0001$) or across

Table 2: Quantitative genetics of sexual size dimorphism at six ages

Trait and age (months)	Sample size (N)		Residual variance (V_E)		Additive genetic variance (V_A)		Heritability (h^2)		Between-sex covariance	Between-sex r_{mf}
	Male	Female	Male	Female	Male	Female	Male	Female		
SVL:										
1	409	436	.00194 ± .00020	.00164 ± .00022	.00018 ± .00016	**.00070 ± .00025**	.084 ± .077	**.300 ± .097**	.00030	**.835 ± .406**
3	357	373	.00341 ± .00034	.00294 ± .00033	.00022 ± .00026	.00043 ± .00030	.061 ± .071	.127 ± .086	.00031	**1**
6	346	373	.00206 ± .00019	.00087 ± .00019	.00015 ± .00013	**.00041 ± .00015**	.067 ± .056	**.321 ± .108**	.00025	**1**
9	298	313	.00223 ± .00023	.00097 ± .00016	.00016 ± .00017	**.00041 ± .00018**	.067 ± .068	**.302 ± .120**	.00026	**1**
12	350	369	.00249 ± .00032	.00084 ± .00011	.00052 ± .00031	**.00031 ± .00012**	.174 ± .099	**.268 ± .100**	.00025	.631 ± .321
24	278	299	.00171 ± .00031	.00086 ± .00016	**.00070 ± .00034**	**.00055 ± .00020**	**.290 ± .131**	**.390 ± .126**	.00023	*.374 ± .279*
Mass:										
1	418	445	.0327 ± .0032	.0309 ± .0034	.0047 ± .0027	**.0085 ± .0035**	.124 ± .071	**.215 ± .083**	.0063	**1**
3	366	385	.0442 ± .0044	.0425 ± .0042	.0025 ± .0033	.0032 ± .0031	.054 ± .070	.069 ± .068	.0028	1
6	359	381	.0200 ± .0022	.0110 ± .0015	.0035 ± .0021	**.0040 ± .0017**	.150 ± .084	**.265 ± .101**	.0037	**1**
9	305	313	.0224 ± .0024	.0121 ± .0016	.0021 ± .0019	.0026 ± .0016	.087 ± .076	.178 ± .102	.0024	**1**
12	351	371	.0307 ± .0035	.0119 ± .0017	.0038 ± .0030	**.0047 ± .0019**	.111 ± .085	**.283 ± .106**	.0025	.598 ± .394
24	284	303	.0224 ± .0035	.0161 ± .0026	**.0069 ± .0036**	**.0068 ± .0029**	**.236 ± .116**	**.297 ± .118**	.0030	*.438 ± .317*

Note: Parameter estimates (±SE) are derived from animal model analysis using a paternal half-sib breeding design. Boldface indicates values of V_A, h^2, and r_{mf} significantly ($P < .05$) greater than 0. Italics indicates r_{mf} values significantly ($P < .05$) less than 1. SVL = snout-vent length.

Table 3: Ontogenetic changes in the quantitative genetic architecture of body size

	SVL		Body mass		
Parameter	*r*	*P*	*r*	*P*	Interpretation
V_{Am}	**.89**	**.018**	.68	.137	Additive genetic variance increases with age in males
V_{Af}	−.12	.816	.13	.802	Additive genetic variance constant with age in females
B	**−.83**	**.042**	−.48	.335	Between-sex genetic covariance decreases with age
h^2_m	**.92**	**.009**	.78	.077	Heritability increases with age in males
h^2_f	.63	.188	.62	.199	Heritability increases slightly with age in females
r_{mf}	**−.84**	**.036**	**−.90**	**.014**	Between-sex genetic correlation decreases with age

Note: Data are Pearson correlations between point estimates of genetic parameters for body size (SVL or body mass) and age (1, 3, 6, 9, 12, or 24 months posthatching), with interpretations regarding ontogenetic patterns in the quantitative genetics of body size. SVL = snout-vent length.

488 genes with sex-biased expression at either age ($r = 0.273$; $P < .0001$).

Functional Enrichment of Sex-Biased Genes

Analyses using GO terms revealed significant enrichment for sex-biased genes in pathways related to metabolism (e.g., GO term = metabolic process; $n = 309$ sex-biased genes; $P = .0026$) and digestion (e.g., GO term = digestion; $n = 18$ sex-biased genes; $P < .0001$; table A2). IPA analysis indicated sex-biased enrichment and activation of mTOR signaling (fig. A1, available online), a pathway that we identified a priori as a focal network for regulation of growth (see below). Pathways with less obvious relevance to growth and body size that were also enriched for sex-biased genes are presented in table A2.

Sex-Biased Expression of Growth-Regulatory Genes

The three gene networks that we selected a priori for their roles in growth, metabolism, and cell proliferation (tables A3–A5) each exhibited significant ontogenetic increases in the magnitude of sex-biased expression: the growth hormone/insulin-like growth factor (GH/IGF) network (Wilcoxon: $S = 49.5$; $n = 16$; $P < .001$; fig. 3*B*), the mechanistic target of rapamycin (mTOR) network ($S = 94.0$; $n = 25$; $P < .005$; fig. 3*C*), and the insulin-signaling network ($S = 383.5$; $n = 78$; $P = .038$; fig. 3*D*). The magnitude of these ontogenetic increases in sex-biased expression for the GH/IGF and mTOR networks exceeded the overall trend across all genes in the liver, whereas the increase in sex-biased expression of the insulin-signaling network was similar to that observed across all genes (fig. 3*B*–3*D*). Combining these three interrelated networks revealed a highly significant ontogenetic increase in the sex-biased expression of 101 genes related to growth, metabolism, and cell proliferation ($S = 1{,}028.5$; $P < .0001$). All genes in these pathways map to autosomes in *A. carolinensis*. Analysis of individual genes in the GH/IGF network corroborated this pattern. In juveniles, only one of 16 GH/IGF genes were sex-biased at an uncorrected threshold of $P < .05$ and none were significant after Bonferroni correction (adjusted threshold: $P < .0031$; table A6).

Table 4: Quantitative genetics of asymptotic growth trajectories in males and females

Trait (sex)	Sample size	Residual variance (V_E)	Additive genetic variance (V_A)	Heritability (h^2)
SVL_∞ (male)	246	.0116 ± .0022	**.0043 ± .0023**	**.271 ± .137**
k (male)	246	.0922 ± .0161	.0278 ± .0166	.232 ± .132
SVL_∞ (female)	278	.0017 ± .0003	**.0006 ± .0003**	**.262 ± .113**
k (female)	278	.0398 ± .0049	.0038 ± .0040	.087 ± .091
Trait 1	**Trait 2**	**Residual covariance**	**Additive genetic covariance**	**Genetic correlation**
SVL_∞ (male)	*k* (male)	−.0282 ± .0057	−.0109	−1
SVL_∞ (female)	*k* (female)	−.0069 ± .0010	−.0001	−.088 ± .518
SVL_∞ (male)	SVL_∞ (female)	…	.0008	.508 ± .336
k (male)	*k* (female)	…	.0070	.678 ± .585
SVL_∞ (male)	*k* (female)	…	−.0013	−.314 ± .542
k (male)	SVL_∞ (female)	…	−.0019	−.468 ± .363

Note: Asymptotic size (SVL_∞) and growth parameter (*k*) describe the shape of von Bertalanffy growth trajectories fitted to size data from individual males and females. Boldface indicates estimates significantly different from 0. Residual covariances are fixed at 0 for between-sex comparisons because the traits are not expressed in the same individual. SVL = snout-vent length.

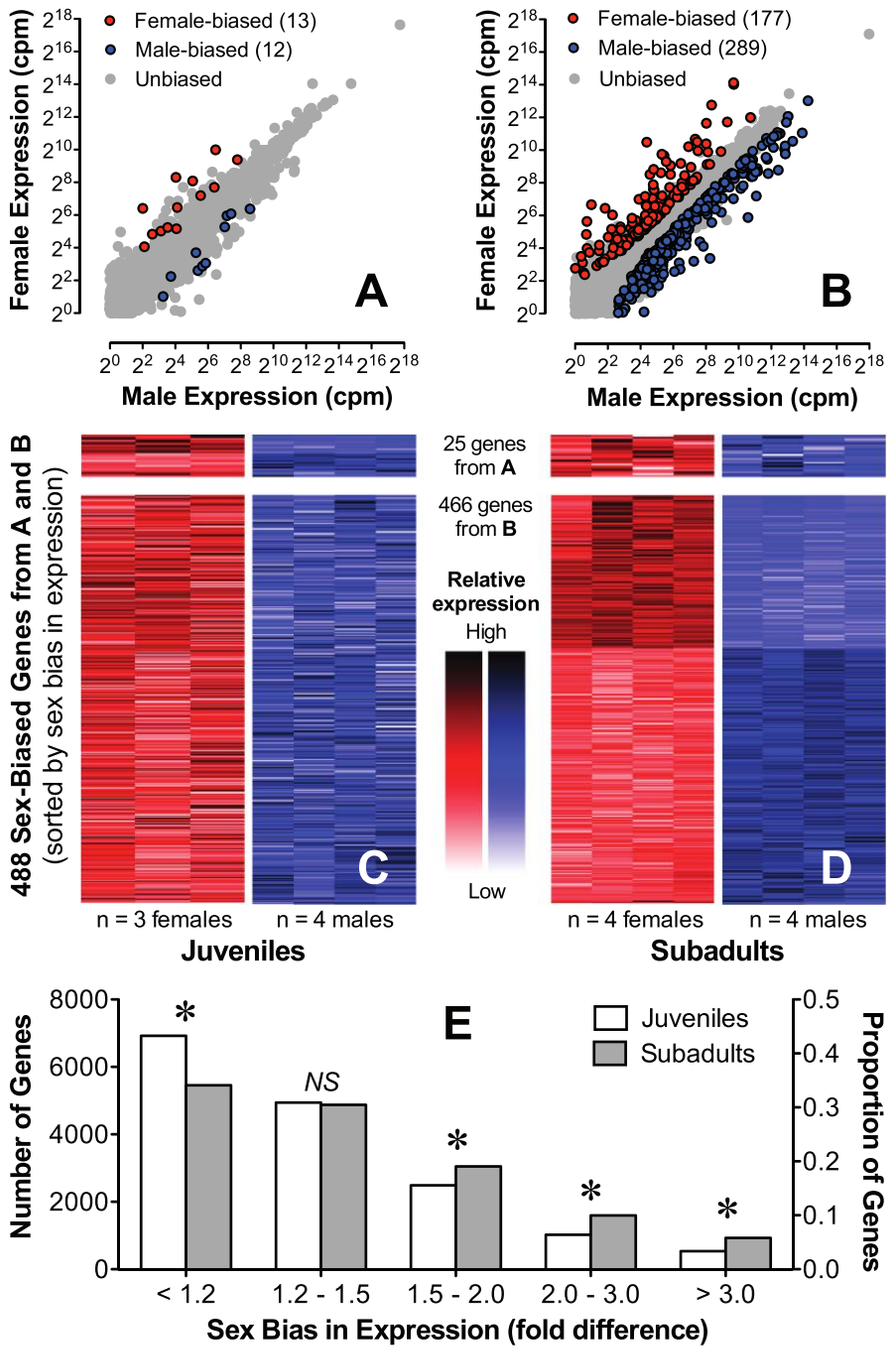

Figure 2: Ontogenetic increases in sex-biased gene expression. *A*, *B*, Mean expression (counts per million) in females versus that in males ($\log_2$ scales) for each of 13,191 expressed genes in juveniles (*A*) and 12,688 expressed genes in subadults (*B*; excluding 6,132 and 6,645 genes with expression below $2^0 = 1$ cpm in juveniles and subadults, respectively). Genes with significantly sex-biased expression (pairwise exact tests correcting for false discovery) are indicated in red (female biased) or blue (male biased). *C*, *D*, Heat maps illustrating expression patterns for these 488 sex-biased genes. Rows correspond to genes, and columns correspond to individuals. Rows are ranked by the mean sex difference in expression in juveniles (*top*, illustrating 25 genes from *A*) or subadults (*bottom*, illustrating 466 genes from *B*). *E*, Distribution of transcriptome-wide sex bias in expression across 15,915 genes binned into five classes based on mean fold difference in expression. Asterisks indicate significant ($P < .0001$) differences between juveniles and subadults in the number of genes in each bin based on χ^2 tests.

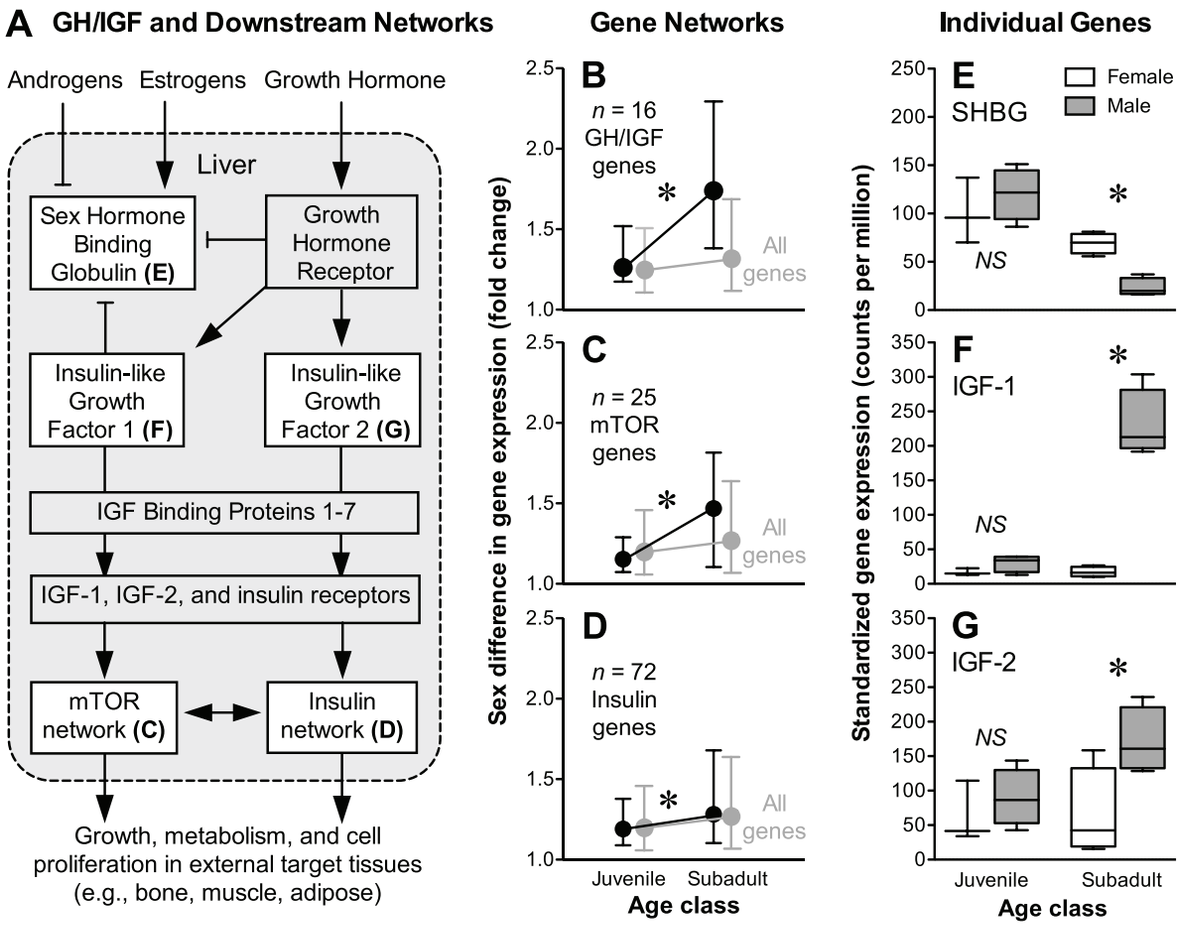

Figure 3: *A*, Simplified schematic of components in the growth hormone/insulin-like growth factor (GH/IGF) pathway and downstream hepatic networks influencing growth, metabolism, and cell proliferation. *B–D*, Median (±interquartile range) fold differences in gene expression between sexes at two ages, shown separately for three gene networks: the GH/IGF network (*B*), the mTOR network (*C*), and the insulin-signaling network (*D*). Asterisks indicate significant increases in the sex-biased expression of each individual network with age, and gray symbols illustrate the corresponding ontogenetic pattern for all liver genes. *E–G*, Box-and-whisker plots illustrating the median (line), 25%–75% interquartile (box), and range (whiskers) of expression for three upstream genes in the GH/IGF network: sex hormone-binding globulin (*E*), insulin-like growth factor 1 (*F*), and insulin-like growth factor 2 (*G*). Asterisks indicate significant ($P < .05$) sex differences in expression at each age.

In subadults, six of 14 expressed GH/IGF genes were sex biased at an uncorrected $P < .05$, and three remained significant after Bonferroni correction: sex hormone-binding globulin (fig. 3*E*), insulin-like growth factor 1 (fig. 3*F*), and insulin-like growth factor 2 (fig. 3*G*).

Response to Testosterone

Treatment of juvenile females with testosterone tended to increase the expression of genes that were significantly male biased in subadults and to decrease the expression of genes that were significantly female biased (Mann-Whitney $U = 13{,}920$; $P < .0001$; fig. 4*A*). These changes were comparable to natural sex differences between juvenile females and control males (fig. 4*A*), and analogous effects of testosterone were also observed across the entire liver transcriptome (fig. 4*B*). Responsiveness to testosterone in juvenile females differed significantly across six categories ranging from high to low male- or female-biased expression in subadults (Kruskal-Wallis $K = 239.5$; $P < .0001$), and the $\log_2$ fold change in response to testosterone in juvenile females explained a low but highly significant proportion of the variance in $\log_2$ fold difference between subadult males and females ($r^2 = 0.06$; $P < .0001$). For genes in the GH/IGF, mTOR, and insulin-signaling pathways, the direction of sex-biased expression in juveniles was similar to that in subadults (fig. 5*A*), and testosterone tended to increase the expression of male-biased genes while decreasing the expression of female-biased genes (Mann-Whitney $U = 924$; $P = .025$; fig. 5*B*). This pattern is illustrated on a gene-by-gene basis using male-biased

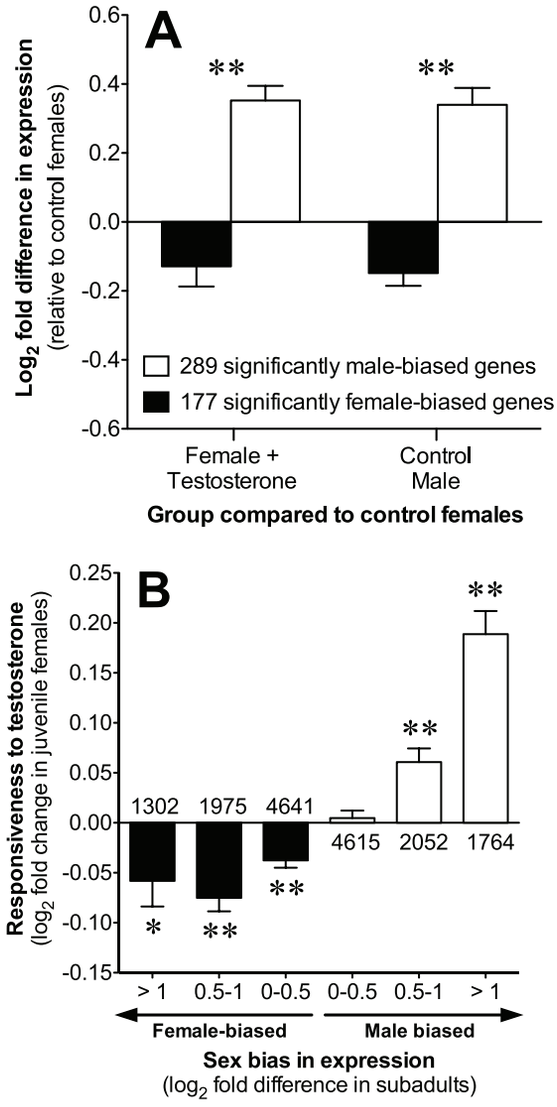

Figure 4: *A*, Mean (±SEM) $\log_2$ fold differences in expression between juvenile female controls and juvenile females treated with testosterone (*left*) or juvenile male controls (*right*) for 466 genes with significantly sex-biased expression in subadults (see fig. 2). Asterisks indicate significant (double: $P < .0001$) differences between male- and female-biased genes based on Mann-Whitney tests. *B*, Mean (±SEM) responsiveness to testosterone in juvenile females ($\log_2$ fold difference between controls and females treated with testosterone) of all expressed genes in the liver, binned into categories corresponding to the magnitude of their sex-biased expression in subadults. Numbers above and below bars indicate the number of genes in each category. Asterisks indicate significant (single: $P < .05$; double: $P < .0001$) differences from 0 within each category based on Wilcoxon signed-rank tests.

genes for several growth factors and their receptors and binding proteins located upstream in the GH/IGF pathway (fig. 5*C*–5*H*). IPA enrichment analyses also identified growth hormone signaling as one of the top pathways activated by testosterone (10 of 81 genes significantly responsive to testosterone; $P = .0003$; table A7).

Data Availability. Illumina RNAseq reads are accessioned at the National Center for Biotechnology Information Short Read Archive (SRX2253414-SRX22534570). Phenotype and pedigree data, as well as short read accession numbers and normalized gene expression matrixes, are accessioned at the Dryad Digital Repository: http://dx.doi.org/10.5061/dryad.n95k3 (Cox et al. 2016*a*).

Discussion

We found that the development of extreme sexual size dimorphism in *Anolis sagrei* was accompanied by the breakdown of r_{mf} for body size as well as a corresponding increase in the sex-biased expression of shared genes in the liver. This increase was particularly pronounced for autosomal genes involved in growth, metabolism, and cell proliferation, strengthening the inference that these regulatory changes are causally related to both the phenotypic development of sexual size dimorphism and the erosion of r_{mf} for body size and growth rate. Moreover, this breakdown of r_{mf} was underlain by a pronounced ontogenetic increase in sex-specific additive genetic variance within males, and patterns of sex-biased gene expression were experimentally inducible by testosterone in females. Collectively, these results suggest that the development of sexual size dimorphism and associated breakdown of r_{mf} may be due in large part to changes in the sex-specific expression of autosomal genes that are ultimately mediated by maturational increases in testosterone levels of males, though further studies are required to causally link patterns of sex-biased and testosterone-mediated gene expression to r_{mf}. The fact that sexual dimorphism in captivity (31% in length, 172% in mass) was similar to levels observed in the wild (32% in length, 153% in mass; Cox et al. 2009*a*; Cox and Calsbeek 2010*b*) suggests that our estimates of r_{mf} provide reasonable approximations of natural patterns. Our estimates are also consistent with a previous study of *A. sagrei* that reported a low r_{mf} for body size using parent-offspring regression (Calsbeek and Bonneaud 2008). Our results provide the most detailed characterization to date of how r_{mf} and its constituent genetic variances and covariances change over ontogeny, as well as the first explicit demonstration of how these developmental changes in genetic architecture occur alongside genome-wide increases in sex-biased gene expression, many of which are also experimentally inducible by testosterone.

The developmental breakdown of r_{mf} appears to be a general feature of sexually dimorphic traits in a variety of taxa (Poissant and Coltman 2009), though r_{mf} can remain high throughout ontogeny for traits that nonetheless develop pronounced sexual dimorphism (Parker and Garant 2005).

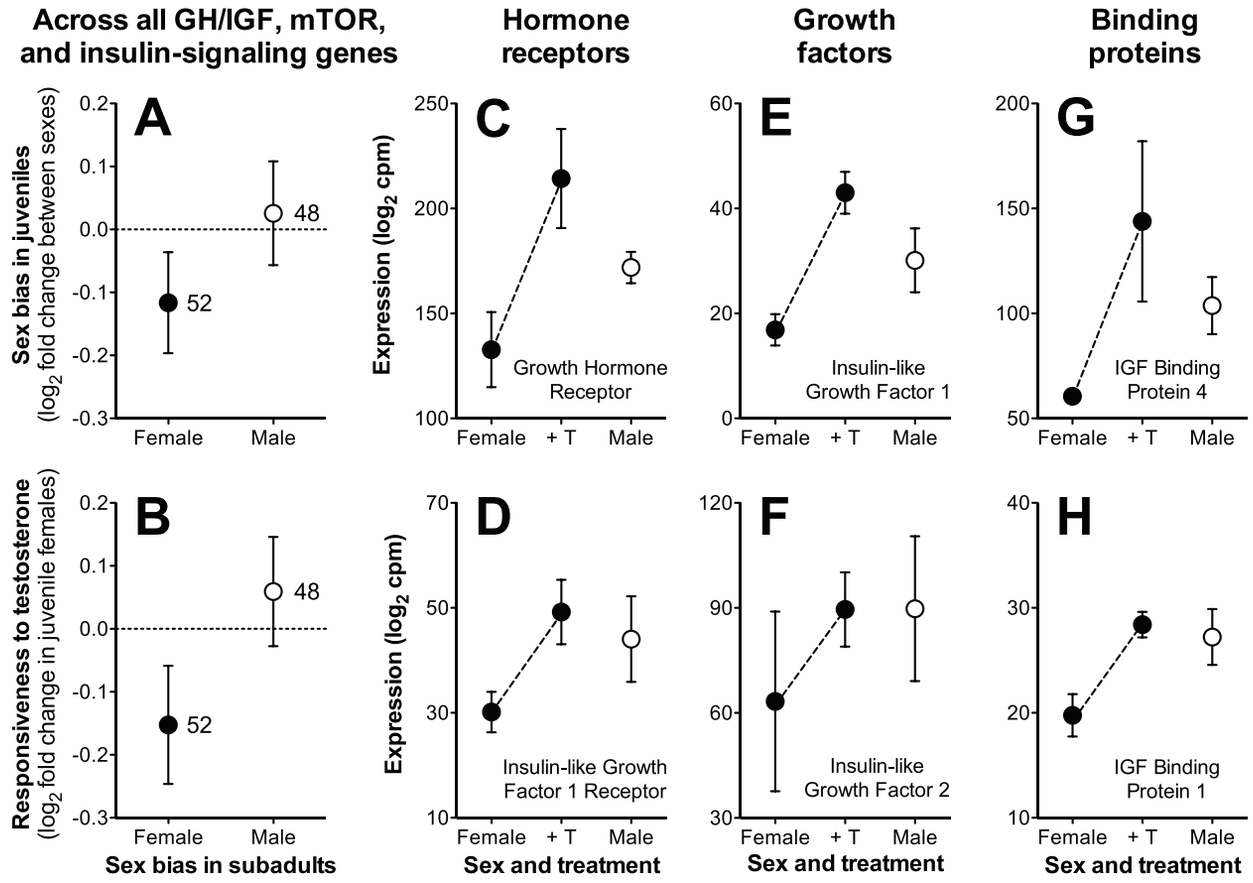

Figure 5: *A*, Mean (±SEM) $\log_2$ fold differences in expression between juvenile males and females for all 100 genes in the GH/IGF, mTOR, and insulin-signaling pathways that could be categorized by their direction of sex-biased expression in subadults (one gene had equivalent expression in subadult males and females and was therefore excluded). *B*, Mean (±SEM) $\log_2$ fold differences in expression between control females and juvenile females treated with testosterone for these same 100 genes. *C–H*, Mean (±SEM) expression of male-biased GH/IGF genes encoding endocrine growth factors, their receptors, and their binding proteins. For these genes, testosterone induced levels of gene expression in juvenile females that matched or exceeded those of juvenile males.

Theoretically, this could occur via the fixation of alleles that are (or will become) entirely sex limited (i.e., inherited or expressed in only one sex) such that they contribute to phenotypic sexual dimorphism without contributing to standing genetic variation in either sex. Our finding that between-sex genetic covariance (*B*) for body size decreased over ontogeny is consistent with the interpretation that many of the same autosomal genes initially contribute to genetic variation for body size in similar ways in each sex, but these shared genes become increasingly sex specific in their translation into phenotypes as ontogeny progresses. We also found that additive genetic variance for (and heritability of) growth and body size increased over ontogeny (table 3). This pattern was particularly pronounced for males, suggesting that the developmental increases in sex-biased gene expression that we observed, which were also highly skewed in favor of male-biased genes (fig. 2*B*), may facilitate the expression of sex-specific additive genetic variance. Fisher (1958) proposed a similar model for the ontogenetic emergence of sex-specific genetic variance, implicating maturational changes in "internal secretions of the sexual glands" as a potential mechanism (Poissant and Coltman 2009). Fisher's view and our data are both consistent with known activational effects of testosterone on growth, body size, and other sexually dimorphic traits in *A. sagrei* (Cox et al. 2009*a*, 2009*b*, 2015). Our transcriptome data provide a first step toward linking these phenotypic and quantitative genetic perspectives by characterizing the changes in gene expression that accompany this emergence of sex-specific genetic variance and demonstrating their responsiveness to testosterone.

We identified 3.1% of transcribed genes in the liver as significantly sex biased in their expression, with the vast majority of these genes encoded on autosomes and biased in subadults rather than in juveniles (fig. 2). Even when we variably excluded each of the four female replicates from our comparison of subadults (to match the sampling design

in our comparison of juveniles; fig. 2), we still detected between 324 and 450 significantly sex-biased genes in subadults, which is more than an order of magnitude greater than in juveniles. We observed a similar pattern when disregarding statistical significance and simply characterizing each gene by its fold difference in expression between the sexes (fig 2*E*). Relative to juveniles, subadults had significantly fewer genes with minor sex bias (<1.2-fold difference) and significantly more genes with major sex bias (>1.5-fold difference). This is not to imply that the liver transcriptome was sexually monomorphic in juveniles. Instead, roughly a quarter of all expressed genes differed by more than 1.5-fold in expression between juvenile males and females (fig. 2*E*), which agrees with the observation that sexual divergence in body size and growth was becoming evident just prior to the age at which we first characterized gene expression (fig. 1). However, sex differences in gene expression became increasingly pronounced as the sexes became increasingly dimorphic in body size and quantitative-genetic architecture. This ontogenetic increase in sex-biased expression was highly skewed in favor of male-biased genes (fig. 2), potentially reflecting their hormonal activation during maturational shifts toward adult male phenotypes, which are highly differentiated from those of juveniles and females. An excess of male-biased (relative to female-biased) genes has also been observed in adults of other species (Peterson et al. 2014), though this trend can vary or reverse across tissues (Yang et al. 2006; Xia et al. 2007) and over ontogeny (Mank et al. 2010; Magnusson et al. 2011; Perry et al. 2014).

Our estimate of 3.1% of hepatic genes exhibiting sex-biased expression falls near the low end of variation observed across other studies (reviewed by Ingleby et al. 2015), with estimates ranging from 2% or fewer sex-biased genes in adult marine snails (Martinez-Fernandez et al. 2010), adult zebra fish brains (Santos et al. 2008), and various tissues from larval and pupal silkworms (Xia et al. 2007) to 90% or more in adult fruit flies (Wayne et al. 2007; Ayroles et al. 2009; Innocenti and Morrow 2010). Presumably, our estimate is conservative due to the lower statistical power associated with three or four individual replicates per sex and age class, though similar replication is typical in transcriptomic surveys of sex bias (Ingleby et al. 2015). At the opposite end of the spectrum, microarray data from an atypically large sample of mice ($n = 169$ females; $n = 165$ males) provided >90% power to detect 5% differences in mean expression between sexes, resulting in estimates ranging from several hundred (brain) to several thousand sex-biased genes (liver, adipose, muscle), with a range of 13% (brain) to 72% (liver) of expressed genes exhibiting a significant sex bias (Yang et al. 2006). However, the majority of these sex-biased genes in mice (71%–94% across tissues) displayed <1.2-fold sex differences in expression (Yang et al. 2006), whereas all of the genes that we identified as sex biased in anoles displayed >1.7-fold sex differences in expression. Though the true percentage of sex-biased genes in the *A. sagrei* liver probably exceeds 3.1%, our approach has the advantage of highlighting large transcriptional biases that may have greater influence on the phenotypic development of sexual dimorphism and the associated breakdown of r_{mf} for body size.

Three regulatory networks that should be particularly relevant to growth and body size are the GH/IGF, mTOR, and insulin-signaling networks, each of which exhibited an increase in sex-biased expression from juveniles to subadults (fig. 3*A*–3*C*). The GH/IGF pathway has long been the focus of research on vertebrate growth (Duan and Xu 2005; Sparkman et al. 2010; McGaugh et al. 2015), and ontogenetic increases in sex-biased expression were particularly pronounced for insulin-like growth factors (IGFs) due to their upregulation in subadult males (fig. 3*E*, 3*F*). IGF-1 is a potent promoter of growth in vertebrates, and increased levels of plasma IGF-1 and hepatic IGF-1 expression are associated with rapid growth and large body size in reptiles (Sparkman et al. 2009, 2010; Duncan et al. 2015). Although IGF-2 is viewed as a specialized regulator of prenatal growth in mammals, patterns of IGF-2 expression and sequence evolution in reptiles suggest that IGF-2 may have a more general role in promoting growth across ontogeny in this group (McGaugh et al. 2015), consistent with our data.

In contrast to the IGFs, sex hormone–binding globulin (SHBG) was strongly downregulated in subadult males (fig. 3*D*), consistent with the mammalian paradigm in which SHBG (which binds and mediates the activity of sex steroids) is stimulated by estrogens but inhibited by androgens. Expression of SHBG was also strongly inhibited by testosterone in our experiment ($t = 4.8$; $P = .009$). The natural suppression of SHBG expression in subadult males thus implies that the increasingly dimorphic expression of growth-regulatory genes may be due in part to maturational changes in circulating androgens (Cox et al. 2009*a*, 2015). Our experimental results directly support this hypothesis by showing that male-biased genes for IGFs and their binding proteins and receptors can be stimulated by treatment of females with exogenous testosterone (fig. 5). Viewed alongside similar ontogenetic increases in the sex-specific regulation of mTOR and insulin-signaling networks (fig. 3), which interact with GH/IGF signaling to influence growth, metabolism, and cell proliferation (McGaugh et al. 2015), these functional links to known growth-regulatory pathways suggest that hormonally mediated shifts in sex-biased gene expression may contribute to both the phenotypic expression of sexual size dimorphism and the developmental breakdown of r_{mf} for body size. The broad congruence between sex-biased expression and responsiveness to testosterone that we observed is similar to expression patterns found in mice, where treatment of females with exogenous androgens induces natural patterns of sex-biased gene expression (Yang et al. 2006; van Nas et al.

2009). The pleiotropic effects of testosterone on gene expression that we observed are also similar to patterns found in juncos (*Junco hyemalis*), where testosterone exerts a combination of shared and sex-specific effects on gene expression and putatively mitigates sexual conflict over a shared genome (Peterson et al. 2013, 2014).

Our data are consistent with the interpretation that hormonally mediated increases in sex-biased gene expression contribute to breakdown of r_{mf}, but they do not directly address the roles of other genetic mechanisms that may facilitate the resolution of intralocus sexual conflict, such as sex linkage (van Doorn and Kirkpatrick 2007; Roberts et al. 2009) or genomic imprinting (Day and Bonduriansky 2004; Bonduriansky 2007). We found that autosomal genes were as likely as X-linked genes to exhibit significant sex bias in *A. sagrei*, and none of the growth-regulatory genes on which we focused maps to sex chromosomes in *Anolis carolinensis*. Because this reference genome is from a female (Alfioldi et al. 2011), we cannot evaluate the contributions of Y-linked genes. Nonetheless, the development of phenotypic sexual dimorphism clearly involves the sex-biased expression of many autosomal genes, though our data cannot directly address the extent to which these changes may be regulated epistatically by sex-linked modifier loci. The fact that these patterns of sex-biased gene expression, sex-specific V_A, and r_{mf} change substantially across ontogeny is generally inconsistent with a simple form of genomic imprinting involving continuous epigenetic silencing throughout ontogeny. However, our findings do not rule out a potential role of genes with ontogenetically variable patterns of sex-specific imprinting (i.e., silenced only at particular ontogenetic stages) or a role of sex-specific imprinting at modifier loci whose epistatic interactions with other genes and pathways are themselves variable across ontogeny (Wolf et al. 2008; Poissant and Coltman 2009). Therefore, sex linkage and genomic imprinting provide examples of two additional mechanisms through which sex-specific modifiers could potentially regulate patterns of sex-biased expression for autosomal genes, analogous to the role we demonstrate for testosterone.

An important caveat to our study is that correlated ontogenetic changes in phenotypic sexual dimorphism and its quantitative genetic architecture and sex-biased gene expression do not directly demonstrate that testosterone-mediated changes in sex-biased gene expression cause the breakdown of r_{mf} for growth and body size. Future work could strengthen this inference by testing for ontogenetic changes in r_{mf} for the expression of the growth-regulatory genes that we have identified as likely candidates due to their sex-biased expression and responsiveness to testosterone, such as those in the GH/IGF pathway. Characterizing h^2 and r_{mf} for circulating testosterone levels (Pavitt et al. 2014; Iserbyt et al. 2015), as well as genetic correlations between testosterone and gene expression, could further clarify these mechanisms. Last, manipulating testosterone in the context of a quantitative-genetic breeding design while confirming associated changes in gene expression would directly test whether this hormone structures r_{mf} for growth and body size by virtue of its effects on gene expression (Cox et al. 2016*b*).

Predicting the evolution of male and female phenotypes in response to sex-specific selection requires estimates of r_{mf} and its underlying components of genetic variance and covariance, which shape the evolutionary response to selection (Lande 1980, 1987; Merilä et al. 1998; Steven et al. 2007; Poissant et al. 2008). The realization that these quantitative-genetic parameters themselves often vary across ontogeny has led to a new appreciation of the shifting efficacy with which sex-specific selection at different life stages is expected to translate into the evolution of sexual dimorphism (Badyaev 2002; Poissant and Coltman 2009). For example, any sex differences in selection on the size of brown anoles at hatching (Cox et al. 2011) are unlikely to impact the evolution of sexual dimorphism due to high r_{mf} for body size at this age (fig. 1). By contrast, differences in natural or sexual selection on adult size (Cox and Calsbeek 2010*b*), with its substantially reduced r_{mf} and increased V_A, have greater potential to influence the evolution of sexual dimorphism. Of course, r_{mf} itself is an evolving property of a population (Delph et al. 2011), so the decline in r_{mf} that we observe across ontogeny could also indicate that sexually antagonistic selection has historically acted more strongly on the size of adults relative to juveniles. In either case, our results are broadly consistent with the view that maturational increases in sex-specific modifiers such as testosterone can pleiotropically regulate sex-biased patterns of gene expression to developmentally restructure underlying genetic correlations between the sexes.

Acknowledgments

H. Donald-Cannon, J. Price, D. Rose, and many University of Virginia (UVA) students cared for our breeding colony. N. Furst, S. Hwang, D. Muraleetharan, A. Russell, and E. Wice assisted with tissue collection and phenotyping. E. D. Brodie III and V. Formica assisted with the collection of wild anoles, which were imported under permits from the Bahamas Environment, Science, and Technology Commission; the Bahamas Ministry of Agriculture; and the United States Fish and Wildlife Service. UVA's Animal Care and Use Committee approved all procedures (protocol 3896). This project was supported by funding from UVA to R.M.C, from Virginia Tech to J.W.M., a National Science Foundation (NSF) Evo-Devo-Eco Network fellowship to C.L.C. (IOS-095551), and an NSF CAREER award to R.M.C. (DEB-1453089). The authors have no conflicts of interest to declare.

Literature Cited

Alfioldi, J., F. D. Palma, M. Grabherr, C. Williams, L. Kong, E. Mauceli, P. Russell, et al. 2011. The genome of the green anole lizard and a comparative analysis with birds and mammals. Nature 477: 587–591.

Ashburner, M., C. A. Ball, J. A. Blake, D. Botstein, H. Butler, J. M. Cherry, A. P. Davis, et al. 2000. Gene ontology: tool for the unification of biology. Nature Genetics 25:25–29.

Ayroles, J. F., M. A. Carbone, E. A. Stone, K. W. Jordan, R. F. Lyman, M. M. Magwire, S. M. Rollmann, et al. 2009. Systems genetics of complex traits in *Drosophila melanogaster*. Nature Genetics 41: 299–307.

Badyaev, A. V. 2002. Growing apart: an ontogenetic perspective on the evolution of sexual size dimorphism. Trends in Ecology and Evolution 17:369–378.

Benjamini, Y., and Y. Hochberg. 1995. Controlling the false discovery rate: a practical and powerful approach to multiple testing. Journal of the Royal Statistical Society B 57:289–300.

Bolger, A. M., M. Lohse, and B. Usadel. 2014. Trimmomatic: a flexible trimmer for Illumina sequence data. Bioinformatics 30:2114–2120.

Bonduriansky, R. 2007. The genetic architecture of sexual dimorphism: the potential roles of genomic imprinting and condition dependence. Pages 176–184 *in* D. J. Fairbairn, W. U. Blanckenhorn, and T. Szekely, eds. Sex, size and gender roles: evolutionary studies of sexual size dimorphism. Oxford University Press, Oxford.

Bonduriansky, R., and S. F. Chenoweth. 2009. Intralocus sexual conflict. Trends in Ecology and Evolution 24:280–288.

Bonduriansky, R., and L. Rowe. 2005. Intralocus sexual conflict and the genetic architecture of sexually dimorphic traits in *Prochyliza xanthostoma* (Diptera: Piophilidae). Evolution 59:1965–1975.

Calsbeek, R., and C. Bonneaud. 2008. Postcopulatory fertilization bias as a form of cryptic sexual selection. Evolution 62:1137–1148.

Chou, C.-C., Y. Iwasa, and T. Nakazawa. 2016. Incorporating an ontogenetic perspective into evolutionary theory of sexual size dimorphism. Evolution 70:369–384.

Connallon, T., and A. G. Clark. 2011. The resolution of sexual antagonism by gene duplication. Genetics 187:919–937.

Cox, C. L., A. F. Hanninen, A. M. Reedy, and R. M. Cox. 2015. Female anoles retain responsiveness to testosterone despite the evolution of androgen-mediated sexual dimorphism. Functional Ecology 29:758–767.

Cox, R. M., and R. Calsbeek. 2009. Sexually antagonistic selection, sexual dimorphism, and the resolution of intralocus sexual conflict. American Naturalist 173:176–187.

———. 2010*a*. Cryptic sex-ratio bias provides indirect genetic benefits despite sexual conflict. Science 328:92–94.

———. 2010*b*. Sex-specific selection and intraspecific variation in sexual size dimorphism. Evolution 64:798–809.

Cox, R. M., C. L. Cox, J. W. McGlothlin, D. C. Card, A. L. Andrew, and T. A. Castoe. 2016*a*. Data from: Hormonally mediated increases in sex-biased gene expression accompany the breakdown of between-sex genetic correlations in a sexually dimorphic lizard. American Naturalist, Dryad Digital Repository, http://dx.doi.org/10.5061/dryad.n95k3.

Cox, R. M., M. C. Duryea, M. Najarro, and R. Calsbeek. 2011. Paternal condition drives progeny sex-ratio bias in a lizard that lacks parental care. Evolution 65:220–230.

Cox, R. M., J. W. McGlothlin, and F. Bonier. 2016*b*. Hormones as mediators of phenotypic and genetic integration: and evolutionary genetics approach. Integrative and Comparative Biology 56:126–137.

Cox, R. M., D. S. Stenquist, and R. Calsbeek. 2009*a*. Testosterone, growth, and the evolution of sexual size dimorphism. Journal of Evolutionary Biology 22:1586–1598.

Cox, R. M., D. S. Stenquist, J. P. Henningsen, and R. Calsbeek. 2009*b*. Manipulating testosterone to assess links between behavior, morphology and performance in the brown anole, *Anolis sagrei*. Physiological and Biochemical Zoology 82:686–698.

Day, T., and R. Bonduriansky. 2004. Intralocus sexual conflict can drive the evolution of genomic imprinting. Genetics 167:1537–1546.

Dean, R., and J. E. Mank. 2016. Tissue specificity and sex-specific regulatory variation permits the evolution of sex-biased gene expression. American Naturalist 188:E74–E84.

Delph, L. F., J. C. Steven, I. A. Anderson, C. R. Herlihy, and E. D. Brodie III. 2011. Elimination of a genetic correlation between the sexes via artificial correlational selection. Evolution 65:2872–2880.

Duan, C., and Q. Xu. 2005. Roles of insulin-like growth factor (IGF) binding proteins in regulating IGF actions. General and Comparative Endocrinology 142:44–52.

Duncan, C. A., A. E. Jetzt, W. S. Cohick, and H. B. John-Alder. 2015. Nutritional modulation of IGF-1 in relation to growth and body condition in *Sceloporus* lizards. General and Comparative Endocrinology 216:116–124.

Ellegren, H., and J. Parsch. 2007. The evolution of sex-biased genes and sex-biased gene expression. Nature Reviews Genetics 8:689–698.

Fairbairn, D. J., and D. A. Roff. 2006. The quantitative genetics of sexual dimorphism: assessing the importance of sex-linkage. Heredity 97:319–328.

Fisher, R. A. 1930. Sexual reproduction and sexual selection: the genetical theory of natural selection. Clarendon, Oxford.

———. 1958. The genetical theory of natural selection. Dover, New York.

Gallach, M., and E. Betrán. 2011. Intralocus sexual conflict resolved through gene duplication. Trends in Ecology and Evolution 26:222–228.

Gilmour, A. R., B. J. Gogel, B. R. Cullis, S. J. Welham, and R. Thompson. 2015. ASReml user guide: functional specification. Version 4.1. VSN, Hemel Hempstead, United Kingdom.

Grath, S., and J. Parsch. 2016. Sex-biased gene expression. Annual Review of Genetics 50:29–44.

Griffin, R. M., R. Dean, J. L. Grace, P. Rydén, and U. Friberg. 2013. The shared genome is a pervasive constraint on the evolution of sex-biased gene expression. Molecular Biology and Evolution 30: 2168–2176.

Harrison, P. W., A. E. Wright, F. Zimmer, R. Dean, S. H. Montgomery, M. A. Pointer, and J. E. Mank. 2015. Sexual selection drives evolution and rapid turnover of male gene expression. Proceedings of the National Academy of Sciences of the USA 112: 4393–4398.

Hollis, B., D. Houle, Z. Yan, T. J. Kawecki, and L. Keller. 2014. Evolution under monogamy feminizes gene expression in *Drosophila melanogaster*. Nature Communications 5:3482.

Ingleby, F. C., I. Flis, and E. H. Morrow. 2015. Sex-biased gene expression and sexual conflict throughout development. Cold Spring Harbor Perspectives in Biology 7:1–17.

Innocenti, P., and E. H. Morrow. 2010. The sexually antagonistic genes of *Drosophila melanogaster*. PLoS Biology 8:e1000335.

Iserbyt, A., M. Eens, and W. Müller. 2015. Sexually antagonistic selection during parental care is not generated by a testosterone-related intralocus sexual conflict: insights from full-sib comparisons. Scientific Reports 5:17715.

Kanehisa, M., and S. Goto. 2000. KEGG: Kyoto encyclopedia of genes and genomes. Nucleic Acids Research 28:27–30.

Kanehisa, M., S. Goto, S. Kawashima, Y. Okuna, and M. Hattori. 2004. The KEGG resource for deciphering the genome. Nucleic Acids Research 32:D277–D280.

Kelder, T., M. P. Van Iersel, K. Hanspers, M. Kutmon, B. R. Conklin, C. T. Evelo, and A. R. Pico. 2011. WikiPathways: building research communities on biological pathways. Nucleic Acids Research 40: D1301–D1307.

Kijimoto, T., A. P. Moczek, and J. Andrews. 2012. Diversification of *doublesex* function underlies morph-, sex-, and species-specific development of beetle horns. Proceedings of the National Academy of Sciences of the USA 109:20526–20531.

Lande, R. 1980. Sexual dimorphism, sexual selection, and adaptation in polygenic characters. Evolution 34:292–307.

———. 1987. Genetic correlations between the sexes in the evolution of sexual dimorphism and mating preferences. Pages 83–94 *in* J. W. Bradbury and M. B. Andersson, eds. Sexual selection: testing the alternatives. Wiley, Chichester, United Kingdom.

Li, H., and R. Durbin. 2009. Fast and accurate short read alignment with Burrows-Wheeler transform. Bioinformatics 25:1754–1760.

Li, H., B. Handsaker, A. Wysoker, T. Fennel, K. Ruan, N. Homer, G. Marth, et al. 2009. The sequence/alignment/map format and SAMtools. Bioinformatics 25:2078–2079.

Magnusson, K., A. M. Mendes, N. Windbichler, P.-A. Papathanos, T. Nolan, T. Dottorini, E. Rizzi, et al. 2011. Transcription regulation of sex-biased genes during ontogeny in the malaria vector *Anopheles gambiae*. PLoS ONE 6:e21572.

Mank, J. E. 2007. The evolution of sexually selected traits and antagonistic androgen expression in actinopterygian fish. American Naturalist 169:142–149.

———. 2009. Sex chromosomes and the evolution of sexual dimorphism: lessons from the genome. American Naturalist 173:141–150.

Mank, J. E., K. Nam, B. Brunström, and H. Ellegren. 2010. Ontogenetic complexity of sexual dimorphism and sex-specific selection. Molecular Biology and Evolution 27:1570–1578.

Martinez-Fernandez, M., L. Bernatchez, E. Rolan-Alvarez, and H. Quesada. 2010. Semi-quantitative differences in gene transcription profiles between sexes of a marine snail by a new variant of cDNA-AFLP analysis. Molecular Ecology Resources 10:324–330.

McGaugh, S. E., A. M. Bronikowski, C.-H. Kuo, D. M. Reding, E. A. Addis, L. E. Flagel, F. J. Janzen, et al. 2015. Rapid molecular evolution across amniotes of the IIS/TOR network. Proceedings of the National Academy of Sciences of the USA 112:7055–7060.

Merilä, J., B. C. Sheldon, and H. Ellegren. 1998. Quantitative genetics of sexual size dimorphism in the collared flycatcher, *Ficedula albicollis*. Evolution 52:870–876.

Mills, S. C., E. Koskela, and T. Mappes. 2012. Intralocus sexual conflict for fitness: sexually antagonistic alleles for testosterone. Proceedings of the Royal Society B 279:1889–1895.

Mokkonen, M., E. Koskela, T. Mappes, and S. C. Mills. 2012. Sexual antagonism for testosterone maintains multiple mating behaviour. Journal of Animal Ecology 81:277–283.

Parker, T. H., and D. Garant. 2005. Quantitative genetics of ontogeny of sexual dimorphism in red junglefowl (*Gallus gallus*). Heredity 95:401–407.

Pavitt, A. T., C. A. Walling, J. M. Pemberton, and L. E. B. Kruuk. 2014. Heritability and cross-sex genetic correlations of early-life circulating testosterone levels in a wild mammal. Biology Letters 10.

Perry, J. C., P. W. Harrison, and J. E. Mank. 2014. The ontogeny and evolution of sex-biased gene expression in *Drosophila melanogaster*. Molecular Biology and Evolution 31:1206–1219.

Peterson, M. P., K. A. Rosvall, J.-H. Choi, C. Ziegenfus, H. Tang, J. K. Colbourne, and E. D. Ketterson. 2013. Testosterone affects neural gene expression differently in male and female juncos: a role for hormones in mediating sexual dimorphism and conflict. PLoS ONE 8:e61784.

Peterson, M. P., K. A. Rosvall, C. A. Taylor, J. A. Lopez, J.-H. Choi, C. Ziegenfus, H. Tang, et al. 2014. Potential for sexual conflict assessed via testosterone-mediated transcriptional changes in liver and muscle of a songbird. Journal of Experimental Biology 217: 507–517.

Pointer, M. A., P. W. Harrison, A. E. Wright, and J. E. Mank. 2013. Masculinization of gene expression is associated with exaggeration of male sexual dimorphism. PLoS Genetics 9:e1003697.

Poissant, J., and D. W. Coltman. 2009. The ontogeny of cross-sex genetic correlations: an analysis of patterns. Journal of Evolutionary Biology 22:2558–2562.

Poissant, J., A. J. Wilson, and D. W. Coltman. 2010. Sex-specific genetic variance and the evolution of sexual dimorphism: a systematic review of cross-sex genetic correlations. Evolution 64:97–107.

Poissant, J., A. J. Wilson, M. Festa-Bianchet, J. T. Hogg, and D. W. Coltman. 2008. Quantitative genetics and sex-specific selection on sexually dimorphic traits in bighorn sheep. Proceedings of the Royal Society B 275:623–628.

Rice, W. R., and A. K. Chippindale. 2001. Intersexual ontogenetic conflict. Journal of Evolutionary Biology 14:865–693.

Roberts, R. B., J. R. Ser, and T. D. Kocher. 2009. Sexual conflict resolved by invasion of a novel sex determiner in Lake Malawi cichlid fishes. Science 326:998–1001.

Robinson, M. D., D. J. McCarthy, and G. K. Smyth. 2010. edgeR: a Bioconductor package for differential expression analysis of digital gene expression data. Bioinformatics 26:139–140.

Santos, E. M., P. Kille, V. L. Workman, G. C. Paull, and C. R. Tyler. 2008. Sexually dimorphic gene expression in the brains of mature zebrafish. Comparative Biochemistry and Physiology A 149:314–324.

Schneider, C. A., W. S. Rasband, and K. W. Eliceiri. 2012. NIH Image to ImageJ: 25 years of image analysis. Nature Methods 9:671–675.

Smedley, D., S. Haider, S. Durinck, L. Pandini, P. Provero, J. Allen, O. Arnaiz, et al. 2015. The BioMart community portal: an innovative alternative to large, centralized data repositories. Nucleic Acids Research 43:W589–W598.

Sparkman, A. M., D. Byars, N. B. Ford, and A. M. Bronikowski. 2010. The role of insulin-like growth factor-1 (IGF-1) in growth and reproduction in female brown house snakes (*Lamprophis fuliginosus*). General and Comparative Endocrinology 168:408–414.

Sparkman, A. M., C. M. Vleck, and A. M. Bronikowski. 2009. Evolutionary ecology of endocrine-mediated life-history variation in the garter snake *Thamnophis elegans*. Ecology 90:720–728.

Steven, J. C., L. F. Delph, and E. D. Brodie. 2007. Sexual dimorphism in the quantitative-genetic architecture of floral, leaf, and allocation traits in *Silene latifolia*. Evolution 61:42–57.

Stewart, A. D., A. Pischedda, and W. R. Rice. 2010. Resolving intralocus sexual conflict: genetic mechanisms and time frame. Journal of Heredity 101:S94–S99.

Stocks, M., R. Dean, B. Rogell, and U. Friberg. 2015. Sex-specific trans-regulatory variation on the *Drosophila melanogaster* x chromosome. PLoS Genetics 11:e1005015.

van Doorn, G. S., and M. Kirkpatrick. 2007. Turnover of sex chromosomes induced by sexual conflict. Nature 449:909–912.

van Nas, A., D. G. Thakurta, S. Wang, N. Yehya, S. Hovarth, B. Zhang, L. Ingram-Drake, et al. 2009. Elucidating the role of gonadal hormones in sexually dimorphic gene coexpression networks. Endocrinology 150:1235–1249.

Wang, J., D. Duncan, Z. Shi, and B. Zhang. 2013. WEB-based GEne SeT AnaLysis Toolkit (WebGestalt): update 2013. Nucleic Acids Research 41:W77–W83.

Wayne, M. L., M. Telonis-Scott, L. M. Bono, L. Harshman, A. Kopp, S. V. Nuzhdin, and L. M. McIntyre. 2007. Simpler mode of inheritance of transcriptional variation in male *Drosophila melanogaster*. Proceedings of the National Academy of Sciences of the USA 104:18577–18582.

Wolf, J. B., J. M. Cheverud, C. Roseman, and R. Hager. 2008. Genome-wide analysis reveals a complex pattern of genomic imprinting in mice. PLoS Genetics 4:e1000091.

Xia, Q., D. Cheng, J. Duan, G. Wang, T. Cheng, X. Zha, C. Liu, et al. 2007. Microarray-based gene expression profiles in multiple tissues of the domesticated silkworm, *Bombyx mori*. Genome Biology 8:R162.

Yang, X., E. E. Schadt, S. Wang, H. Wang, A. P. Arnold, L. Ingram-Drake, T. A. Drake, et al. 2006. Tissue-specific expression and regulation of sexually dimorphic genes in mice. Genome Research 16: 995–1004.

Zhang, B., S. Kirov, and J. Snoddy. 2005. WebGestalt: an integrated system for exploring gene sets in various biological contexts. Nucleic Acids Research 33:W741–W748.

Zhao, M., X.-F. Zha, J. Liu, W.-J. Zhang, N.-J. He, D.-J. Cheng, Y. Dai, et al. 2011. Global expression profile of silkworm genes from larval to pupal stages: toward a comprehensive understanding of sexual differences. Insect Science 18:607–618.

Associate Editor: Russell Bonduriansky
Editor: Yannis Michalakis

An adult male brown anole (*Anolis sagrei*). Photo credit: Ariel Kahrl.